

# Search for Lepton Flavor Violating $\tau^-$ Decays into $\ell^- K_S^0$ and $\ell^- K_S^0 K_S^0$

Y. Miyazaki,<sup>25</sup> I. Adachi,<sup>8</sup> H. Aihara,<sup>47</sup> K. Arinstein,<sup>1,34</sup> V. Aulchenko,<sup>1,34</sup>  
A. M. Bakich,<sup>42</sup> V. Balagura,<sup>13</sup> E. Barberio,<sup>24</sup> A. Bay,<sup>20</sup> K. Belous,<sup>10</sup> M. Bischofberger,<sup>26</sup>  
A. Bozek,<sup>30</sup> M. Bračko,<sup>22,14</sup> T. E. Browder,<sup>7</sup> M.-C. Chang,<sup>4</sup> P. Chang,<sup>29</sup> A. Chen,<sup>27</sup>  
K.-F. Chen,<sup>29</sup> P. Chen,<sup>29</sup> B. G. Cheon,<sup>6</sup> I.-S. Cho,<sup>51</sup> Y. Choi,<sup>41</sup> M. Danilov,<sup>13</sup>  
M. Dash,<sup>50</sup> Z. Doležal,<sup>2</sup> A. Drutskoy,<sup>3</sup> W. Dungel,<sup>11</sup> S. Eidelman,<sup>1,34</sup> N. Gabyshev,<sup>1,34</sup>  
P. Goldenzweig,<sup>3</sup> B. Golob,<sup>21,14</sup> H. Ha,<sup>18</sup> J. Haba,<sup>8</sup> K. Hara,<sup>25</sup> K. Hayasaka,<sup>25</sup>  
H. Hayashii,<sup>26</sup> Y. Horii,<sup>46</sup> Y. Hoshi,<sup>45</sup> W.-S. Hou,<sup>29</sup> Y. B. Hsiung,<sup>29</sup> H. J. Hyun,<sup>19</sup>  
T. Iijima,<sup>25</sup> K. Inami,<sup>25</sup> M. Iwabuchi,<sup>51</sup> M. Iwasaki,<sup>47</sup> Y. Iwasaki,<sup>8</sup> T. Julius,<sup>24</sup>  
D. H. Kah,<sup>19</sup> J. H. Kang,<sup>51</sup> P. Kapusta,<sup>30</sup> N. Katayama,<sup>8</sup> T. Kawasaki,<sup>32</sup> C. Kiesling,<sup>23</sup>  
H. J. Kim,<sup>19</sup> H. O. Kim,<sup>19</sup> J. H. Kim,<sup>17</sup> Y. J. Kim,<sup>5</sup> B. R. Ko,<sup>18</sup> P. Krokovny,<sup>8</sup>  
R. Kumar,<sup>36</sup> A. Kuzmin,<sup>1,34</sup> Y.-J. Kwon,<sup>51</sup> S.-H. Kyeong,<sup>51</sup> M. J. Lee,<sup>40</sup> S.-H. Lee,<sup>18</sup>  
J. Li,<sup>7</sup> C. Liu,<sup>39</sup> D. Liventsev,<sup>13</sup> R. Louvot,<sup>20</sup> A. Matyja,<sup>30</sup> S. McOnie,<sup>42</sup> H. Miyata,<sup>32</sup>  
R. Mizuk,<sup>13</sup> G. B. Mohanty,<sup>43</sup> T. Mori,<sup>25</sup> M. Nakao,<sup>8</sup> H. Nakazawa,<sup>27</sup> Z. Natkaniec,<sup>30</sup>  
S. Nishida,<sup>8</sup> O. Nitoh,<sup>49</sup> S. Ogawa,<sup>44</sup> T. Ohshima,<sup>25</sup> S. Okuno,<sup>15</sup> S. L. Olsen,<sup>40,7</sup>  
G. Pakhlova,<sup>13</sup> H. K. Park,<sup>19</sup> M. Petrič,<sup>14</sup> L. E. Piilonen,<sup>50</sup> A. Poluektov,<sup>1,34</sup> M. Röhrken,<sup>16</sup>  
S. Ryu,<sup>40</sup> H. Sahoo,<sup>7</sup> Y. Sakai,<sup>8</sup> O. Schneider,<sup>20</sup> K. Senyo,<sup>25</sup> M. E. Sevier,<sup>24</sup>  
M. Shapkin,<sup>10</sup> C. P. Shen,<sup>7</sup> J.-G. Shiu,<sup>29</sup> B. Shwartz,<sup>1,34</sup> J. B. Singh,<sup>36</sup> P. Smerkol,<sup>14</sup>  
A. Sokolov,<sup>10</sup> S. Stanič,<sup>33</sup> M. Starič,<sup>14</sup> T. Sumiyoshi,<sup>48</sup> S. Suzuki,<sup>38</sup> M. Tanaka,<sup>8</sup>  
Y. Teramoto,<sup>35</sup> K. Trabelsi,<sup>8</sup> T. Tsuboyama,<sup>8</sup> S. Uehara,<sup>8</sup> S. Uno,<sup>8</sup> Y. Usov,<sup>1,34</sup>  
G. Varner,<sup>7</sup> K. Vervink,<sup>20</sup> C. H. Wang,<sup>28</sup> J. Wang,<sup>37</sup> P. Wang,<sup>9</sup> X. L. Wang,<sup>9</sup>  
M. Watanabe,<sup>32</sup> Y. Watanabe,<sup>15</sup> E. Won,<sup>18</sup> B. D. Yabsley,<sup>42</sup> H. Yamamoto,<sup>46</sup>  
Y. Yamashita,<sup>31</sup> Z. P. Zhang,<sup>39</sup> V. Zhilich,<sup>1,34</sup> A. Zupanc,<sup>16</sup> and O. Zyukova<sup>1,34</sup>

(The Belle Collaboration)

<sup>1</sup>*Budker Institute of Nuclear Physics, Novosibirsk, Russian Federation*

<sup>2</sup>*Faculty of Mathematics and Physics,*

*Charles University, Prague, The Czech Republic*

<sup>3</sup>*University of Cincinnati, Cincinnati, OH, USA*

<sup>4</sup>*Department of Physics, Fu Jen Catholic University, Taipei, Taiwan*

<sup>5</sup>*The Graduate University for Advanced Studies, Hayama, Japan*

<sup>6</sup>*Hanyang University, Seoul, South Korea*

<sup>7</sup>*University of Hawaii, Honolulu, HI, USA*

<sup>8</sup>*High Energy Accelerator Research Organization (KEK), Tsukuba, Japan*

<sup>9</sup>*Institute of High Energy Physics, Chinese Academy of Sciences, Beijing, PR China*

<sup>10</sup>*Institute for High Energy Physics, Protvino, Russian Federation*

<sup>11</sup>*Institute of High Energy Physics, Vienna, Austria*

<sup>12</sup>*INFN - Sezione di Torino, Torino, Italy*

<sup>13</sup>*Institute for Theoretical and Experimental Physics, Moscow, Russian Federation*

<sup>14</sup>*J. Stefan Institute, Ljubljana, Slovenia*

<sup>15</sup>*Kanagawa University, Yokohama, Japan*

- <sup>16</sup>*Institut für Experimentelle Kernphysik,  
Karlsruhe Institut für Technologie, Karlsruhe, Germany*
- <sup>17</sup>*Korea Institute of Science and Technology Information, Daejeon, South Korea*
- <sup>18</sup>*Korea University, Seoul, South Korea*
- <sup>19</sup>*Kyungpook National University, Taegu, South Korea*
- <sup>20</sup>*École Polytechnique Fédérale de Lausanne, EPFL, Lausanne, Switzerland*
- <sup>21</sup>*Faculty of Mathematics and Physics,  
University of Ljubljana, Ljubljana, Slovenia*
- <sup>22</sup>*University of Maribor, Maribor, Slovenia*
- <sup>23</sup>*Max-Planck-Institut für Physik, München, Germany*
- <sup>24</sup>*University of Melbourne, Victoria, Australia*
- <sup>25</sup>*Nagoya University, Nagoya, Japan*
- <sup>26</sup>*Nara Women's University, Nara, Japan*
- <sup>27</sup>*National Central University, Chung-li, Taiwan*
- <sup>28</sup>*National United University, Miao Li, Taiwan*
- <sup>29</sup>*Department of Physics, National Taiwan University, Taipei, Taiwan*
- <sup>30</sup>*H. Niewodniczanski Institute of Nuclear Physics, Krakow, Poland*
- <sup>31</sup>*Nippon Dental University, Niigata, Japan*
- <sup>32</sup>*Niigata University, Niigata, Japan*
- <sup>33</sup>*University of Nova Gorica, Nova Gorica, Slovenia*
- <sup>34</sup>*Novosibirsk State University, Novosibirsk, Russian Federation*
- <sup>35</sup>*Osaka City University, Osaka, Japan*
- <sup>36</sup>*Panjab University, Chandigarh, India*
- <sup>37</sup>*Peking University, Beijing, PR China*
- <sup>38</sup>*Saga University, Saga, Japan*
- <sup>39</sup>*University of Science and Technology of China, Hefei, PR China*
- <sup>40</sup>*Seoul National University, Seoul, South Korea*
- <sup>41</sup>*Sungkyunkwan University, Suwon, South Korea*
- <sup>42</sup>*School of Physics, University of Sydney, NSW 2006, Australia*
- <sup>43</sup>*Tata Institute of Fundamental Research, Mumbai, India*
- <sup>44</sup>*Toho University, Funabashi, Japan*
- <sup>45</sup>*Tohoku Gakuin University, Tagajo, Japan*
- <sup>46</sup>*Tohoku University, Sendai, Japan*
- <sup>47</sup>*Department of Physics, University of Tokyo, Tokyo, Japan*
- <sup>48</sup>*Tokyo Metropolitan University, Tokyo, Japan*
- <sup>49</sup>*Tokyo University of Agriculture and Technology, Tokyo, Japan*
- <sup>50</sup>*IPNAS, Virginia Polytechnic Institute and State University, Blacksburg, VA, USA*
- <sup>51</sup>*Yonsei University, Seoul, South Korea*

## Abstract

We have searched for the lepton-flavor-violating decays  $\tau^- \rightarrow \ell^- K_S^0$  and  $\ell^- K_S^0 K_S^0$  ( $\ell = e$  or  $\mu$ ), using a data sample of  $671 \text{ fb}^{-1}$  collected with the Belle detector at the KEKB asymmetric-energy  $e^+e^-$  collider. No evidence for a signal was found in any of the decay modes, and we set the following upper limits for the branching fractions:  $\mathcal{B}(\tau^- \rightarrow e^- K_S^0) < 2.6 \times 10^{-8}$ ,  $\mathcal{B}(\tau^- \rightarrow \mu^- K_S^0) < 2.3 \times 10^{-8}$ ,  $\mathcal{B}(\tau^- \rightarrow e^- K_S^0 K_S^0) < 7.1 \times 10^{-8}$  and  $\mathcal{B}(\tau^- \rightarrow \mu^- K_S^0 K_S^0) < 8.0 \times 10^{-8}$  at the 90% confidence level.

PACS numbers: 11.30.Fs; 13.35.Dx; 14.60.Fg

## INTRODUCTION

Lepton flavor violation (LFV) in charged lepton decays is forbidden in the Standard Model (SM) or highly suppressed if neutrino mixing is included. However, LFV appears in various extensions of the SM. In particular, the lepton-flavor-violating decays  $\tau^- \rightarrow \ell^- K_S^0$  and  $\tau^- \rightarrow \ell^- K_S^0 K_S^0$  (where  $\ell = e$  or  $\mu$ ) are enhanced in supersymmetric and many other models [1–6]. Some of these models predict branching fractions which, for certain combinations of model parameters, can be as high as  $10^{-7}$ ; this level is already accessible in high-statistics  $B$ -factory experiments. Previously, we obtained 90% confidence level (C.L.) upper limits for the  $\tau^- \rightarrow \ell^- K_S^0$  branching fractions ( $\mathcal{B}$ ) using  $281 \text{ fb}^{-1}$  of data; the results were  $\mathcal{B}(\tau^- \rightarrow e^- K_S^0) < 5.6 \times 10^{-8}$  and  $\mathcal{B}(\tau^- \rightarrow \mu^- K_S^0) < 4.9 \times 10^{-8}$  [7]. The BaBar collaboration has recently obtained 90% C.L. upper limits of  $\mathcal{B}(\tau^- \rightarrow e^- K_S^0) < 3.3 \times 10^{-8}$  and  $\mathcal{B}(\tau^- \rightarrow \mu^- K_S^0) < 4.0 \times 10^{-8}$  using a data sample of  $469 \text{ fb}^{-1}$  [8]. The most restrictive existing upper limits  $\mathcal{B}(\tau^- \rightarrow e^- K_S^0 K_S^0) < 2.2 \times 10^{-6}$  and  $\mathcal{B}(\tau^- \rightarrow \mu^- K_S^0 K_S^0) < 3.4 \times 10^{-6}$  at the 90% C.L. were set by the CLEO experiment using  $13.9 \text{ fb}^{-1}$  of data [9]. In this paper, we present a search for the lepton-flavor-violating decays  $\tau^- \rightarrow \ell^- K_S^0$  and  $\ell^- K_S^0 K_S^0$  ( $\ell = e$  or  $\mu$ ) [†] using  $671 \text{ fb}^{-1}$  of data collected at the  $\Upsilon(4S)$  resonance and 60 MeV below with the Belle detector at the KEKB asymmetric-energy  $e^+e^-$  collider [10].

The Belle detector is a large-solid-angle magnetic spectrometer that consists of a silicon vertex detector (SVD), a 50-layer central drift chamber (CDC), an array of aerogel threshold Cherenkov counters (ACC), a barrel-like arrangement of time-of-flight scintillation counters (TOF), and an electromagnetic calorimeter comprised of CsI(Tl) crystals (ECL), all located inside a superconducting solenoid coil that provides a 1.5 T magnetic field. An iron flux-return located outside of the coil is instrumented to detect  $K_L^0$  mesons and to identify muons (KLM). The detector is described in detail elsewhere [11].

Leptons are identified using likelihood ratios calculated from the responses of various detector subsystems. For electron identification, the likelihood ratio is defined as  $\mathcal{P}(e) = \mathcal{L}_e / (\mathcal{L}_e + \mathcal{L}_x)$ , where  $\mathcal{L}_e$  and  $\mathcal{L}_x$  are the likelihoods for electron and non-electron hypotheses, respectively, determined using the ratio of the energy deposit in the ECL to the momentum measured in the SVD and CDC, the shower shape in the ECL, the matching between the position of the charged track trajectory and the cluster position in the ECL, the hit information from the ACC, and the  $dE/dx$  information in the CDC [12]. For muon identification, the likelihood ratio is defined as  $\mathcal{P}(\mu) = \mathcal{L}_\mu / (\mathcal{L}_\mu + \mathcal{L}_\pi + \mathcal{L}_K)$ , where  $\mathcal{L}_\mu$ ,  $\mathcal{L}_\pi$  and  $\mathcal{L}_K$  are the likelihoods for the muon, pion and kaon hypotheses, respectively, based on the matching quality and penetration depth of associated hits in the KLM [13]. For this measurement, we use hadron identification likelihood variables based on the hit information from the ACC, the  $dE/dx$  information in the CDC, and the particle time-of-flight from the TOF. To distinguish hadron species, we use likelihood ratios,  $\mathcal{P}(i/j) = \mathcal{L}_i / (\mathcal{L}_i + \mathcal{L}_j)$ , where  $\mathcal{L}_i$  ( $\mathcal{L}_j$ ) is the likelihood for the detector response to a track with flavor hypothesis  $i$  ( $j$ ).

In order to optimize the event selection and estimate the signal efficiency, we use Monte Carlo (MC) samples. The signal and background events from generic  $\tau^+\tau^-$  decays are generated by KKMC/TAUOLA [14]. The signal MC samples are generated by KKMC assuming a phase space model for the  $\tau$  decay. Other backgrounds, including  $B\bar{B}$  and continuum  $e^+e^- \rightarrow q\bar{q}$  ( $q = u, d, s, c$ ) events, Bhabha events, and two-photon processes, are generated by EvtGen [15], BHLUMI [16], and AAFH [17], respectively. The Belle detector response

---

[†] Unless otherwise stated, charge-conjugate decays are included throughout this paper.

is simulated by a GEANT 3 [18] based program. The event selection is optimized mode-by-mode since the backgrounds are mode dependent. All kinematic variables are calculated in the laboratory frame unless otherwise specified. In particular, variables calculated in the  $e^+e^-$  center-of-mass (CM) system are indicated by the superscript “CM”.

## DATA ANALYSIS

We search for  $\tau^+\tau^-$  events, in which one  $\tau$  (signal side) decays into  $\ell K_S^0$  or  $\ell K_S^0 K_S^0$ , while the other  $\tau$  (tag side) decays into a final state with one charged track, any number of additional photons and neutrinos. We reconstruct each  $K_S^0$  meson candidate from a  $\pi^+\pi^-$  pair. By selecting decays into one charged track on the tag side, we reduce background from  $B\bar{B}$  and  $q\bar{q}$  events. All charged tracks and photons are required to be reconstructed within a fiducial volume, defined by  $-0.866 < \cos\theta < 0.956$ , where  $\theta$  is the polar angle with respect to the direction opposite to the  $e^+$  beam. We select charged tracks with momenta transverse to the  $e^+$  beam  $p_t > 0.1$  GeV/ $c$  and photons with energies  $E_\gamma > 0.1$  GeV.

Candidate  $\tau$ -pair events are required to have four or six charged tracks with zero net charge for the  $\ell K_S^0$  and  $\ell K_S^0 K_S^0$  modes, respectively. Events are separated into two hemispheres corresponding to the signal (three-prong and five-prong for the  $\ell K_S^0$  and  $\ell K_S^0 K_S^0$  modes, respectively) and tag (one-prong) sides by the plane perpendicular to the thrust axis [19].

We require one or two  $K_S^0$  candidates for the  $\ell K_S^0$  and  $\ell K_S^0 K_S^0$  modes, respectively. The  $K_S^0$  is reconstructed from two oppositely charged tracks on the signal side that have an invariant mass  $0.482 \text{ GeV}/c^2 < M_{\pi^+\pi^-} < 0.514 \text{ GeV}/c^2$ , assuming the pion mass for both tracks. The  $\pi^+\pi^-$  vertex is required to be displaced from the interaction point (IP) in the direction of the pion pair momentum [20]. In order to avoid fake  $K_S^0$  candidates from photon conversions (i.e.,  $\gamma \rightarrow e^+e^-$ ), the invariant mass reconstructed by assigning the electron mass to the tracks, is required to be greater than  $0.2 \text{ GeV}/c^2$ . The electron and muon identification criteria are  $\mathcal{P}(e) > 0.9$  with momentum  $p > 0.3 \text{ GeV}/c$  and  $\mathcal{P}(\mu) > 0.9$  with  $p > 0.6 \text{ GeV}/c$ , respectively. In order to take into account the emission of bremsstrahlung photons from the electron, the momentum of each electron track is reconstructed by adding the momentum of every photon within 0.05 rad of the track direction. The electron (muon) identification efficiency for the  $\ell K_S^0$  modes is 92% (87%) and that for the  $\ell K_S^0 K_S^0$  modes is 79% (81%). The difference of efficiencies between  $\ell K_S^0$  and  $\ell K_S^0 K_S^0$  is due to the different signal momentum distributions. The probability to misidentify a pion as an electron and a muon is below 0.5% and 3%, respectively.

In order to suppress background from  $q\bar{q}$  events, the following requirements on the number of the photon candidates on the signal and tag side ( $n_\gamma^{\text{SIG}}$  and  $n_\gamma^{\text{TAG}}$ ) are imposed:  $n_\gamma^{\text{SIG}} \leq 1$  and  $n_\gamma^{\text{TAG}} \leq 3$ . For the  $\ell K_S^0$  modes only, we also require  $n_\gamma^{\text{TAG}} \leq 1$  if the track of the tag side is a lepton to reduce the background, in particular from  $D^+ \rightarrow \ell^+ \nu K_S^0 (\rightarrow \pi^0 \pi^0)$ .

To ensure that the missing particles are neutrinos rather than photons or charged particles that fall outside the detector acceptance, we impose additional requirements on the missing momentum vector,  $\vec{p}_{\text{miss}}$ , calculated by subtracting the vector sum of the momenta of all tracks and photons from the sum of the  $e^+$  and  $e^-$  beam momenta. We require that the magnitude of  $\vec{p}_{\text{miss}}$  be greater than  $0.4 \text{ GeV}/c$  and that its direction point into the fiducial volume of the detector. Since neutrinos are emitted only on the tag side, the direction of  $\vec{p}_{\text{miss}}$  should lie within the tag side of the event. The cosine of the opening angle between  $\vec{p}_{\text{miss}}$  and the tag-side track in the CM system,  $\cos\theta_{\text{tag-miss}}^{\text{CM}}$ , should be  $0.0 < \cos\theta_{\text{tag-miss}}^{\text{CM}}$

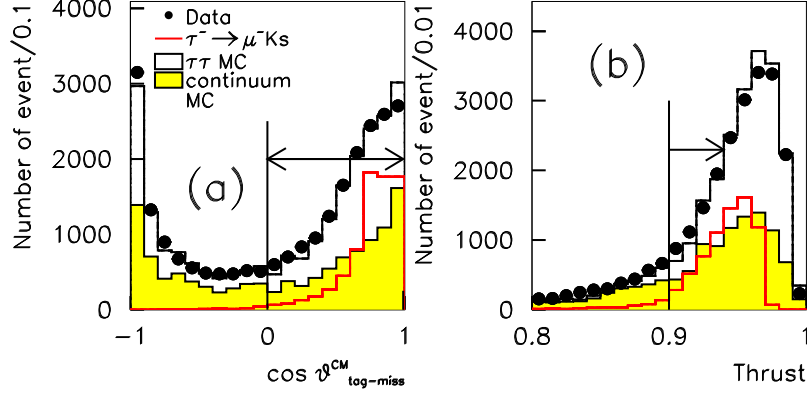


FIG. 1: Kinematic distributions used in the event selection of the  $\tau^- \rightarrow \mu^- K_S^0$  mode: (a) the cosine of the opening angle between a charged track on the tag side and the missing momentum in the CM system ( $\cos \theta_{\text{tag-miss}}^{\text{CM}}$ ); and (b) the magnitude of the thrust. The signal MC ( $\tau^- \rightarrow \mu^- K_S^0$ ) distributions with arbitrary normalization are shown for comparison; the background MC distributions are normalized to the data luminosity. Selected regions are indicated by the arrows from the marked cut boundaries.

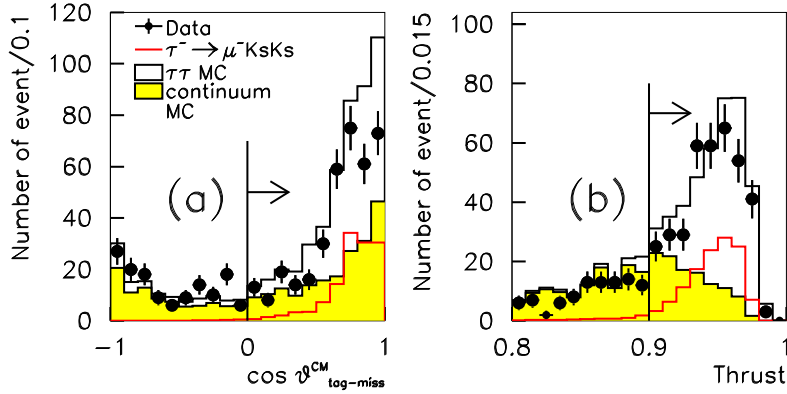


FIG. 2: Kinematic distributions used in the event selection of the  $\tau^- \rightarrow \mu^- K_S^0 K_S^0$  mode: (a) the cosine of the opening angle between a charged track on the tag side and the missing momentum in the CM system ( $\cos \theta_{\text{tag-miss}}^{\text{CM}}$ ); and (b) the magnitude of the thrust. The signal MC ( $\tau^- \rightarrow \mu^- K_S^0 K_S^0$ ) distributions with arbitrary normalization are shown for comparison; the background MC distributions are normalized to the data luminosity. Selected regions are indicated by the arrows from the marked cut boundaries.

for both modes (see Figs. 1 (a) and 2 (a)). For the  $\ell K_S^0$  modes, we also require that  $\cos \theta_{\text{tag-miss}}^{\text{CM}} < 0.99$  to reduce background from Bhabha,  $\mu^+ \mu^-$  and two-photon events, as radiated photons from the tag-side track result in missing momentum if they overlap with the ECL clusters associated with the tag-side track.

To reject the  $q\bar{q}$  background, the magnitude of the thrust is required to be larger than



TABLE I: The selection criteria for the missing momentum ( $p_{\text{miss}}$ ) and missing mass squared ( $m_{\text{miss}}^2$ ) correlations, where  $p_{\text{miss}}$  is in GeV/c and  $m_{\text{miss}}^2$  is in (GeV/c<sup>2</sup>)<sup>2</sup>.

| Modes              | Hadronic tag  | Leptonic tag   |
|--------------------|---|--|
| $\ell K_S^0$       | $p_{\text{miss}} > -3.0 \times m_{\text{miss}}^2 - 0.9$ | $p_{\text{miss}} > -4 \times m_{\text{miss}}^2 - 1.0$  |
|                    | $p_{\text{miss}} > 3.5 \times m_{\text{miss}}^2 - 1.1$  | $p_{\text{miss}} > 1.8 \times m_{\text{miss}}^2 - 0.8$ |
| $\ell K_S^0 K_S^0$ | $p_{\text{miss}} > -2 \times m_{\text{miss}}^2 - 1.0$   | $p_{\text{miss}} > -2 \times m_{\text{miss}}^2 - 1.0$  |
|                    | $p_{\text{miss}} > 2 \times m_{\text{miss}}^2 - 1.0$    | $p_{\text{miss}} > 1.3 \times m_{\text{miss}}^2 - 0.8$ |

0.9 (see Fig. 1 (b) and 2 (b)). The invariant mass reconstructed from the charged track and any photon on the tag side is required to be less than 1.0 and 1.777 GeV/c<sup>2</sup> for the  $\ell K_S^0$  and  $\ell K_S^0 K_S^0$  modes, respectively. For the  $\ell K_S^0$  modes, we impose a kaon veto  $\mathcal{L}(K/\pi) < 0.6$  if the track on the tag side is a hadron, to suppress  $e^+e^- \rightarrow q\bar{q}$  background; due to the conservation of strangeness by the strong interaction, the  $K_S^0$  in such events is often accompanied by another kaon.

All kinematic distributions for the  $\ell K_S^0$  modes shown in Fig. 1 are in reasonable agreement between data and background MC while those for the  $\ell K_S^0 K_S^0$  modes shown in Fig. 2 clearly differ. This difference between the data and background MC in Fig. 2 originates from our poor knowledge of the branching fractions  $\mathcal{B}(\tau^- \rightarrow \pi^- K_S^0 K_S^0 \nu_\tau) = (2.4 \pm 0.5) \times 10^{-4}$  and  $\mathcal{B}(\tau^- \rightarrow \pi^- K^0 \bar{K}^0 \pi^0 \nu_\tau) \times (\mathcal{B}(K^0 \rightarrow K_S^0))^2 = (3.1 \pm 2.3) \times 10^{-4} \times 1/4$  and the dynamics of these decays [21]. Since the final estimate of the background uses information from the data, this discrepancy does not directly affect our results.

Finally, to suppress backgrounds from generic  $\tau^+\tau^-$  and  $q\bar{q}$  events, we apply a selection based on the magnitude of the missing momentum  $p_{\text{miss}}$  and the missing mass squared  $m_{\text{miss}}^2$ . The latter is defined as  $E_{\text{miss}}^2 - p_{\text{miss}}^2$ , where  $E_{\text{miss}} = E_{\text{total}} - E_{\text{vis}}$ ,  $E_{\text{total}}$  is the sum of the beam energies and  $E_{\text{vis}}$  is the total visible energy. We apply different selection criteria depending on the type of one-prong tag: the number of emitted neutrinos is two if the tagging track is an electron or muon (leptonic tag) while it is one if the tagging track is a hadron (hadronic tag). The requirements are listed in Table I (see also Fig. 3).

## RESULTS

Signal candidates are examined in two-dimensional plots of the  $\ell K_S^0$  and  $\ell K_S^0 K_S^0$  invariant mass,  $M_{\text{sig}}$  ( $= M_{\ell K_S^0}, M_{\ell K_S^0 K_S^0}$ ), and the difference of their energy from the beam energy in the CM system,  $\Delta E$ . A signal event should have  $M_{\text{sig}}$  close to the  $\tau$ -lepton mass and  $\Delta E$  close to zero. For both modes, the  $M_{\text{sig}}$  and  $\Delta E$  resolutions are parameterized from the MC distributions around the peak region using asymmetric Gaussian shapes to take into account initial state radiation. The widths of these Gaussians are shown in Table II.

To evaluate the branching fractions, we use an elliptical signal region that contains 90% of the signal MC events satisfying all selection criteria. The shape of the signal region is chosen to minimize its area and therefore obtain the highest sensitivity. We blind the data in the signal region until all selection criteria are finalized so as not to bias our choice of selection criteria. Figure 4 shows scatter-plots for data events and signal MC samples distributed over  $\pm 20\sigma$  in the  $M_{\text{sig}} - \Delta E$  plane. As MC simulation shows, the dominant background in the signal region comes from events with a fake lepton from a pion. Therefore, we estimate the number of expected background by multiplying the number of data events in the signal

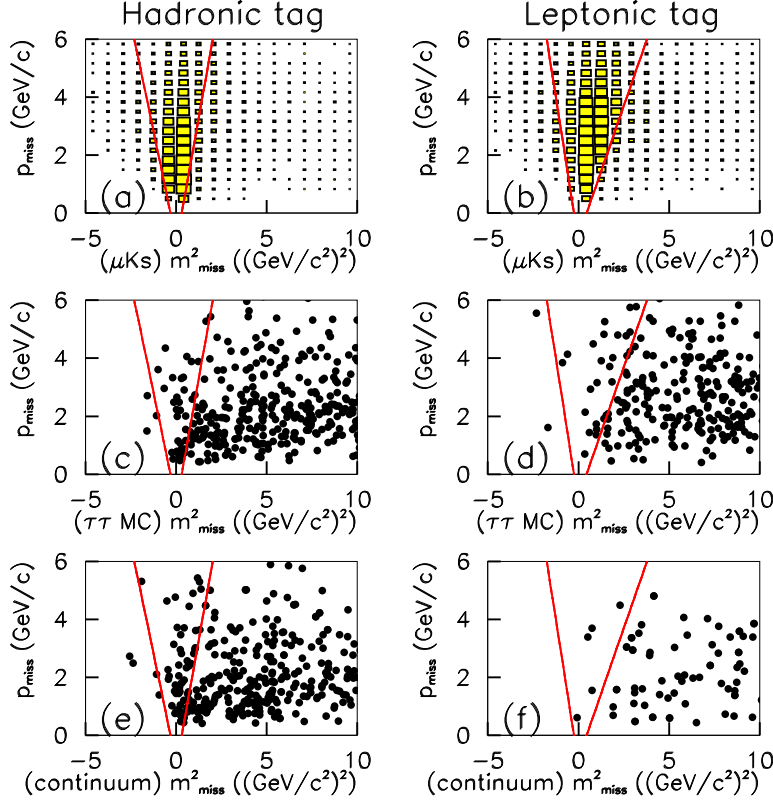


FIG. 3: Scatter-plots of  $p_{\text{miss}}$  vs.  $m_{\text{miss}}^2$ : (a), (c) and (e) show the signal MC ( $\tau^- \rightarrow \mu^- K_S^0$ ), the generic  $\tau^+\tau^-$  MC and  $q\bar{q}$  distributions, respectively, for the hadronic tags while (b), (d) and (f) show the same distributions for the leptonic tags. Selected regions are indicated by lines.

region with selected hadrons ( $\mathcal{P}(\ell) \leq 0.9$ ) by the fake lepton ratio. The latter is calculated as the number of events in the data with  $P(\ell) > 0.9$  divided by the number of events in the data with  $P(\ell) \leq 0.9$  in the sideband region. For the  $\ell K_S^0$  modes we define the sideband region as the box inside the two horizontal lines (see Fig. 4 (a) and (b)) with the signal region excluded since real leptons from  $D^+ \rightarrow \ell^+ \nu K_S^0$  populate the region below the  $\Delta E$  signal one. For the  $\ell K_S^0 K_S^0$  modes, events that lie within a  $\pm 20\sigma$  region but outside the signal region are treated as sideband events (see Fig. 4 (c) and (d)). The final signal efficiency and the number of expected background events in the signal region for each mode are summarized in Table III.

The dominant systematic uncertainties on the detection sensitivity come from  $K_S^0$  reconstruction and tracking efficiencies. These are 4.5% per  $K_S^0$  candidate and 1.0% per track. Other sources of systematic uncertainties are: lepton identification (2.2–2.7)%, MC statistics (0.8–1.0)%, trigger efficiency (0.01–0.4)%, and integrated luminosity (1.4%). The uncertainty from  $\mathcal{B}(K_S^0 \rightarrow \pi^+\pi^-)$  is negligible. All these uncertainties are added in quadrature to provide total systematic uncertainties that range from 6.6% to 11.3%.

Finally, we examine the blinded region and find no data events in the signal region for any of the decay modes (see Fig. 4). Therefore, we set the following upper limits on the



TABLE II: Summary of  $M_{\text{sig}}$  and  $\Delta E$  resolutions ( $\sigma_{M_{\text{sig}}}^{\text{high/low}}$  (MeV/ $c^2$ ) and  $\sigma_{\Delta E}^{\text{high/low}}$  (MeV)). Here  $\sigma^{\text{high}}$  ( $\sigma^{\text{low}}$ ) means the standard deviation on the higher (lower) side of the peak.

| Mode                                   | $\sigma_{M_{\text{sig}}}^{\text{high}}$ | $\sigma_{M_{\text{sig}}}^{\text{low}}$ | $\sigma_{\Delta E}^{\text{high}}$ | $\sigma_{\Delta E}^{\text{low}}$ |
|--|---|--|-----------------------------------|----------------------------------|
| $\tau^- \rightarrow e^- K_S^0$         | 7.3                                     | 7.5                                    | 19.4                              | 30.0                             |
| $\tau^- \rightarrow \mu^- K_S^0$       | 6.2                                     | 6.8                                    | 19.1                              | 26.4                             |
| $\tau^- \rightarrow e^- K_S^0 K_S^0$   | 5.6                                     | 6.4                                    | 12.6                              | 21.9                             |
| $\tau^- \rightarrow \mu^- K_S^0 K_S^0$ | 5.2                                     | 6.0                                    | 11.2                              | 17.2                             |

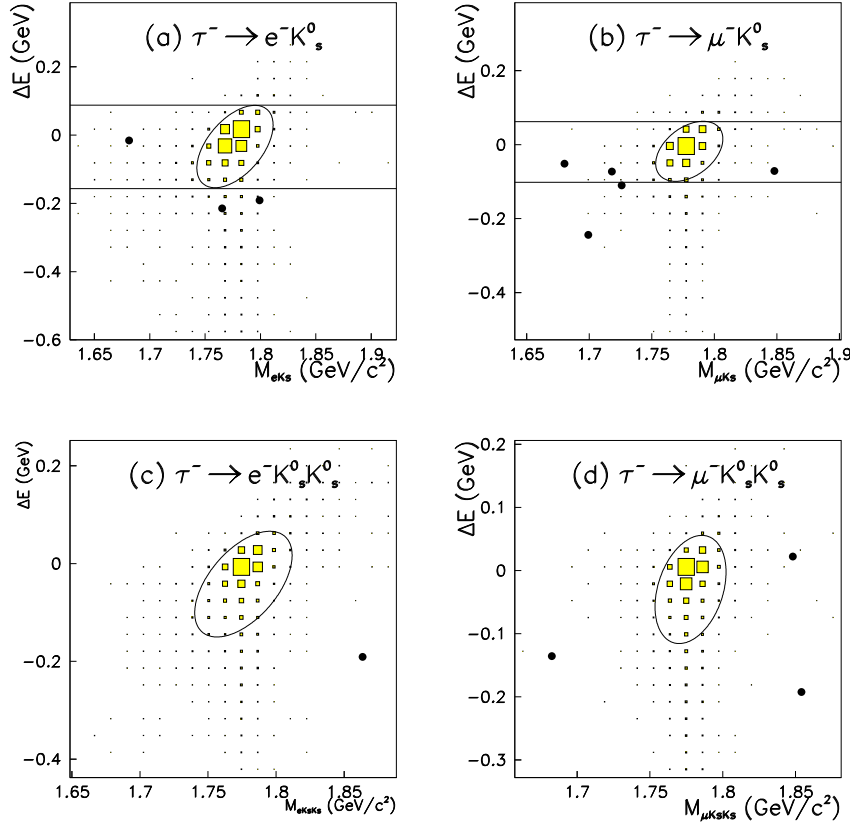


FIG. 4: Scatter-plots of data in the  $M_{\text{sig}} - \Delta E$  plane: (a), (b), (c) and (d) correspond to the  $\pm 20\sigma$  area for the  $\tau^- \rightarrow e^- K_S^0$ ,  $\tau^- \rightarrow \mu^- K_S^0$ ,  $\tau^- \rightarrow e^- K_S^0 K_S^0$  and  $\tau^- \rightarrow \mu^- K_S^0 K_S^0$  modes, respectively. Data is indicated by the solid circles. The filled boxes show the MC signal distribution with arbitrary normalization. The elliptical signal regions shown by the solid curves are used for evaluating the signal yield. In (a) and (b), the region between the horizontal solid lines excluding the signal region is used as a sideband.

TABLE III: The signal efficiency ( $\varepsilon$ ), the number of the expected background events ( $N_{\text{BG}}$ ) estimated from the sideband data, the total systematic uncertainty ( $\sigma_{\text{syst}}$ ), the number of observed events in the signal region ( $N_{\text{obs}}$ ), 90% C.L. upper limit on the number of signal events including systematic uncertainties ( $s_{90}$ ) and 90% C.L. upper limit on the branching fraction for each individual mode.

| Mode   | $\varepsilon$ (%) | $N_{\text{BG}}$ | $\sigma_{\text{syst}}$ (%) | $N_{\text{obs}}$ | $s_{90}$ | $\mathcal{B} (\times 10^{-8})$ |
|--|-------------------|-----------------|----------------------------|------------------|----------|--------------------------------|
| $\tau^- \rightarrow e^- K_{\text{S}}^0$                  | 10.2              | $0.18 \pm 0.18$ | 6.6                        | 0                | 2.25     | $< 2.6$                        |
| $\tau^- \rightarrow \mu^- K_{\text{S}}^0$                | 10.7              | $0.35 \pm 0.21$ | 6.8                        | 0                | 2.10     | $< 2.3$                        |
| $\tau^- \rightarrow e^- K_{\text{S}}^0 K_{\text{S}}^0$   | 5.82              | $0.07 \pm 0.07$ | 11.2                       | 0                | 2.44     | $< 7.1$                        |
| $\tau^- \rightarrow \mu^- K_{\text{S}}^0 K_{\text{S}}^0$ | 5.08              | $0.12 \pm 0.08$ | 11.3                       | 0                | 2.40     | $< 8.0$                        |

branching fractions based on the Feldman-Cousins method [22]. The 90% C.L. upper limit on the number of signal events ( $s_{90}$ ) is obtained using the POLE program [23], based on the number of expected background events, observed data and the systematic uncertainty. The upper limit on the branching fraction is then given by

$$\mathcal{B}(\tau^- \rightarrow \ell^- K_{\text{S}}^0(K_{\text{S}}^0)) < \frac{s_{90}}{2\varepsilon \mathcal{B}(K_{\text{S}}^0 \rightarrow \pi^+ \pi^-)^n N_{\tau\tau}}, \quad (1)$$

where  $\varepsilon$  is the signal efficiency,  $\mathcal{B}(K_{\text{S}}^0 \rightarrow \pi^+ \pi^-) = (69.20 \pm 0.5)\%$  [21], and  $n$  is 1 and 2 for the  $\ell K_{\text{S}}^0$  and  $\ell K_{\text{S}}^0 K_{\text{S}}^0$  modes, respectively. The value  $N_{\tau\tau} = 6.17 \times 10^8$  is obtained from the product of the integrated luminosity and the cross section of  $\tau$ -pair production  $0.919 \pm 0.003$  nb [24]. The resulting upper limits on the branching fractions at the 90% C.L. are

$$\begin{aligned} \mathcal{B}(\tau^- \rightarrow e^- K_{\text{S}}^0) &< 2.6 \times 10^{-8}, \\ \mathcal{B}(\tau^- \rightarrow \mu^- K_{\text{S}}^0) &< 2.3 \times 10^{-8}, \\ \mathcal{B}(\tau^- \rightarrow e^- K_{\text{S}}^0 K_{\text{S}}^0) &< 7.1 \times 10^{-8}, \\ \mathcal{B}(\tau^- \rightarrow \mu^- K_{\text{S}}^0 K_{\text{S}}^0) &< 8.0 \times 10^{-8}. \end{aligned}$$

For the  $\ell K_{\text{S}}^0$  modes, these results improve the existing upper limits by about a factor of 2, compared to our previously published limits [7]. For the  $\ell K_{\text{S}}^0 K_{\text{S}}^0$  modes, these results improve the upper limits by factors of 31 and 43 for the  $e K_{\text{S}}^0 K_{\text{S}}^0$  and  $\mu K_{\text{S}}^0 K_{\text{S}}^0$ , respectively, compared to the previously published limits obtained by the CLEO experiment [9].

## SUMMARY

We have searched for the lepton-flavor-violating decays  $\tau^- \rightarrow \ell^- K_{\text{S}}^0$  and  $\ell^- K_{\text{S}}^0 K_{\text{S}}^0$  ( $\ell = e$  or  $\mu$ ) using data collected with the Belle detector at the KEKB  $e^+e^-$  asymmetric-energy collider. We find no signal for any decay modes. The following upper limits on branching fractions at the 90% confidence level are obtained:  $\mathcal{B}(\tau^- \rightarrow e^- K_{\text{S}}^0) < 2.6 \times 10^{-8}$ ,  $\mathcal{B}(\tau^- \rightarrow \mu^- K_{\text{S}}^0) < 2.3 \times 10^{-8}$ ,  $\mathcal{B}(\tau^- \rightarrow e^- K_{\text{S}}^0 K_{\text{S}}^0) < 7.1 \times 10^{-8}$  and  $\mathcal{B}(\tau^- \rightarrow \mu^- K_{\text{S}}^0 K_{\text{S}}^0) < 8.0 \times 10^{-8}$ . These results are currently the most stringent upper limits for the  $\ell K_{\text{S}}^0$  and the  $\ell K_{\text{S}}^0 K_{\text{S}}^0$  modes. These limits can be used to constrain new physics scenarios beyond the Standard Model.

## Acknowledgments

We are grateful to M. Herrero for useful discussions. We thank the KEKB group for the excellent operation of the accelerator, the KEK cryogenics group for the efficient operation of the solenoid, and the KEK computer group and the National Institute of Informatics for valuable computing and SINET3 network support. We acknowledge support from the Ministry of Education, Culture, Sports, Science, and Technology (MEXT) of Japan, the Japan Society for the Promotion of Science (JSPS), and the Tau-Lepton Physics Research Center of Nagoya University; the Australian Research Council and the Australian Department of Industry, Innovation, Science and Research; the National Natural Science Foundation of China under contract No. 10575109, 10775142, 10875115 and 10825524; the Ministry of Education, Youth and Sports of the Czech Republic under contract No. LA10033; the Department of Science and Technology of India; the BK21 and WCU program of the Ministry Education Science and Technology, National Research Foundation of Korea, and NSDC of the Korea Institute of Science and Technology Information; the Polish Ministry of Science and Higher Education; the Ministry of Education and Science of the Russian Federation and the Russian Federal Agency for Atomic Energy; the Slovenian Research Agency; the Swiss National Science Foundation; the National Science Council and the Ministry of Education of Taiwan; and the U.S. Department of Energy. This work is supported by a Grant-in-Aid from MEXT for Science Research in a Priority Area (“New Development of Flavor Physics”), and from JSPS for Creative Scientific Research (“Evolution of Tau-lepton Physics”).

- 
- [1] A. Ilakovac, Phys. Rev. D **62**, 036010 (2000).
  - [2] D. Black *et al.*, Phys. Rev. D **66**, 053002 (2002).
  - [3] J. P. Saha and A. Kundu, Phys. Rev. D **66**, 054021 (2002).
  - [4] R. Barbier *et al.*, Phys. Rep. **420**, 1 (2005).
  - [5] E. Arganda *et al.*, JHEP **0806**, 079 (2008).
  - [6] Z. H. Li, Y. Li and H. X. Xu, Phys. Lett. B **677**, 150 (2009).
  - [7] Y. Miyazaki *et al.* (Belle Collaboration), Phys. Lett. B **639**, 159 (2006).
  - [8] B. Aubert *et al.* (BaBar Collaboration), Phys. Rev. D **79**, 012004 (2009).
  - [9] S. Chen *et al.* (CLEO Collaboration), Phys. Rev. D **66**, 071101 (2002).
  - [10] S. Kurokawa and E. Kikutani, Nucl. Instr. and Meth. A **499**, 1 (2003), and other papers included in this Volume.
  - [11] A. Abashian *et al.* (Belle Collaboration), Nucl. Instr. and Meth. A **479**, 117 (2002).
  - [12] K. Hanagaki *et al.*, Nucl. Instr. and Meth. A **485**, 490 (2002).
  - [13] A. Abashian *et al.*, Nucl. Instr. and Meth. A **491**, 69 (2002).
  - [14] S. Jadach *et al.*, Comp. Phys. Commun. **130**, 260 (2000).
  - [15] D. J. Lange, Nucl. Instr. and Meth. A **462**, 152 (2001).
  - [16] S. Jadach *et al.*, Comp. Phys. Commun. **70**, 305 (1992).
  - [17] F. A. Berends *et al.*, Comp. Phys. Commun. **40**, 285 (1986).
  - [18] R. Brun *et al.*, GEANT 3.21 CERN Report No. DD/EE/84-1, 453.
  - [19] S. Brandt *et al.*, Phys. Lett. **12**, 57 (1964); E. Farhi, Phys. Rev. Lett. **39**, 1587 (1977).
  - [20] K. Sumisawa *et al.* (Belle Collaboration), Phys. Rev. Lett. **95**, 061801 (2005).
  - [21] C. Amsler *et al.* (Particle Data Group), Phys. Lett. B **667**, 1 (2008).

- [22] G.J. Feldman and R.D. Cousins, Phys. Rev. D **57**, 3873 (1998).
- [23] J. Conrad *et al.*, Phys. Rev. D **67**, 012002 (2003).
- [24] S. Banerjee *et al.*, Phys. Rev. D **77**, 054012 (2008).